Influence of Substrates on the Nucleation and Growth Behaviors of $Ge_2Sb_2Te_5$ Films by Combined Plasma-Enhanced Atomic Layer and Chemical Vapor Deposition

Byung Joon Choi,[†] Seol Choi,[†] Taeyong Eom,[†] Seung Wook Ryu,[†] Deok-Yong Cho,[†] Jaeyeong Heo, Hyeong Joon Kim,[†] Cheol Seong Hwang,*[,†] Yoon Jung Kim,[‡] and Suk Kyoung Hong[‡]

Department of Materials Science and Engineering and Inter-university Semiconductor Research Center, Seoul National University, Seoul 151-744, Korea, and Research & Development division, Hynix Semiconductor Incorporation, Ichon 467-701, Korea

Received December 14, 2008. Revised Manuscript Received February 21, 2009

This study concerned the effect of the substrate on the nucleation and growth behavior of $Ge_2Sb_2Te_5$ (GST) thin films deposited by a combination of plasma-enhanced chemical vapor deposition (for Sb and Te) and plasma-enhanced atomic layer deposition (for Ge) processes at wafer temperatures ranging from 100 to 200 °C using $Ge(i\text{-}C_4H_9)_4$, $Sb(i\text{-}C_3H_7)_3$, and $Te(i\text{-}C_3H_7)_2$ as the Ge, Sb, and Te precursors, respectively. Several oxide and nitride layers that were formed on the Si substrate were concerned as substrates. The nucleation of the GST films on the SiO_2, Si_3N_4, and ZrO_2 substrates was seriously retarded (long incubation cycles) compared to those on the TiN and TiO_2 substrates, where smooth film growth with negligible incubation cycles was achieved. The GST film did not grow at all on the HfO_2 substrate. The reason for the enhanced nucleation and growth properties of GST on the TiO_2 and TiN (partially oxidized) substrates was related to the formation of a GeO_2 phase and the charge exchange effect of a partially reduced Ti oxide. On the other hand, the SiO_2 surface remained insulating during deposition, which inhibited GST nucleation. The different nucleation behaviors also influenced the crystallization behavior of the film, which in turn altered the saturated film growth rates. It is believed that the crystallized GST surface reduced the activation energy for the chemisorption of the precursors, which enhanced the saturated growth rate.

I. Introduction

Chemical vapor deposition (CVD) and atomic layer deposition (ALD) or a combination of the growth methods for phase changing $Ge_2Sb_2Te_5$ (GST) thin films has attracted considerable attention from the semiconductor memory field considering its key role in the fabrication of highly integrated phase change random access memory devices (PcRAM).[1−3] ALD is generally preferred over CVD for the deposition of such complex multicomponent thin films considering its self-regulating growth nature. However, there are no reports of genuine ALD-type growth of GST thin films because of the lack of suitable precursors and reaction (reducing) agents.[3−10] The authors previously reported the growth process of GST films using a combination of plasma-enhanced CVD (PECVD, for Sb and Te) and plasma-enhanced ALD (PEALD, for Ge), where the quality of the grown films was quite promising.[4−6] Nevertheless, because of the complex surface structure onto which the films are deposited, the adoption of a combined PECVD/PEALD process for depositing GST films in the fabrication of the PcRAM requires a more in-depth understanding of the growth behavior depending on the type of substrate and resulting crystalline quality of the films. It was reported that GST film growth by the combined PECVD/PEALD process has serious substrate dependency.[5,6] Although it has not been reported for GST films, the serious influence of electrical conductivity of the substrate (or buffer layer) on the growth of metallic films has been reported.[11,12]

* To whom correspondence should be addressed. E-mail: cheolsh@snu.ac.kr.
[†] Seoul National University.
[‡] Hynix Semiconductor Incorporation.

(1) Lam, C. Presented at *New non-volatile memory workshop 2007*, Hsinchu, Taiwan, November 2007 (unpublished).
(2) Hudgens, S. Presented at *IEEE Non-volatile semiconductor memory workshop 2007*, Monterey, CA, August 2007 (unpublished).
(3) Lee, J. I.; Park, H.; Cho, S. L.; Park, Y. L.; Bae, B. J.; Park, J. H.; Park, J. S.; An, H. G.; Bae, J. S.; Ahn, D. H.; Kim, Y. T.; Horii, H.; Song, S. A.; Shin, J. C.; Park, S. O.; Kim, H. S.; Chung, U-In.; Moon, J. T.; Ryu, B. I. *Symposium on VLSI Technology Tech. Dig.* **2007**, 102.
(4) Choi, B. J.; Choi, S.; Shin, Y. C.; Hwang, C. S.; Lee, J. W.; Jeong, J.; Kim, Y. J.; Hwang, S. Y.; Hong, S. K. *J. Electrochem. Soc.* **2007**, *154*, H318.
(5) Choi, B. J.; Choi, S.; Shin, Y. C.; Kim, K. M.; Hwang, C. S.; Kim, Y. J.; Son, Y. J.; Hong, S. K. *Chem. Mater.* **2007**, *19*, 4387.
(6) Choi, B. J.; Oh, S. H.; Choi, S.; Eom, T.; Shin, Y. C.; Kim, K. M.; Yi, K.-W.; Hwang, C. S.; Kim, Y. J.; Park, H. C.; Baek, T. S.; Hong, S. K. *J. Electrochem. Soc.* **2009**, *156*, H59.
(7) Kim, R.-Y.; Kim, H.-G.; Yoon, S.-G. *Appl. Phys. Lett.* **2006**, *89*, 102107.
(8) Abrutis, A.; Plausinaitiene, V.; Skapas, M.; Wiemer, C.; Salicio, O.; Pirovano, A.; Varesi, E.; Rushworth, S.; Gawelda, W.; Siegel, J. *Chem. Mater.* **2008**, *20*, 3557.
(9) Lee, J.; Choi, S.; Lee, C.; Kang, Y.; Kim, D. *Appl. Surf. Sci.* **2007**, *253*, 3969.
(10) Longo, M.; Salicio, O.; Wiemer, C.; Fallica, R.; Molle, A.; Fanciulli, M.; Giesen, C.; Seitzinger, B.; Baumann, P. K.; Heuken, M.; Rushworth, S. *J. Cryst. Growth* **2008**, *310*, 5053.
(11) Kodas, T. T.; Hampden-Smith, M. J. *The chemistry of metal CVD*; VCH publishers: New York, 1994.
(12) Gladfelter, W. L. *Chem. Mater.* **1993**, *5*, 1372.

10.1021/cm803369b CCC: $40.75
Published on Web 05/12/2009

It appears that charge exchange between the growing film and substrate has a significant influence on the growth behavior of some metallic films.

GST could be a conductor (degenerate semiconductor) when it is crystallized or an insulator when it is amorphous. Therefore, the phase of the growing film can have a significant influence on the growth rate itself, even though other parameters, such as the chemical composition and growth temperature, are invariant. In addition, the appropriate growth temperature range (100−200 °C) for this combined PECVD/PEALD process coincides with the crystallization temperature of the GST thin films. Other complications can originate from the different nucleation and crystallization behaviors of the GST film on substrates of different types. Therefore, the growth kinetics of the GST film is very complicated and requires a thorough experimental procedure to correctly understand it.

This study concerned the nucleation and growth behaviors of GST films on Si substrates with the various nucleation or buffer layers. It was found that the type of substrate has a crucial influence on the nucleation behavior as well as the chemical composition of the film. The different nucleation behaviors also influenced the crystallization behavior of the film, which in turn altered the growth rate of the film even after the substrate effect was masked by the GST film. More insight into the film growth process was achieved from a comparison between the growth behavior of single component and compound films.

II. Experimental Procedure

GST films were deposited using a shower-head type 8-in.-scale plasma-enhanced ALD reactor (Quros Co., Plus-200) at wafer temperatures ranging from 110 to 200 °C. For the investigation of the nucleation and growth behaviors of the GST films on different types of substrates, the deposition temperature was fixed at 150 °C. Tetraisobutyl germanium (TIBGe, Ge(i-C_4H_9)$_4$), triisopropyl antimony (TIPSb, Sb(i-C_3H_7)$_3$), and diisopropyl tellurium (DIPTe, Te(i-C_3H_7)$_2$) were used as the Ge, Sb, and Te precursors, respectively. Ge was deposited using an ALD-like reaction while Sb and Te were deposited using a CVD-like reaction.[5] The precursor purge and precursor injection times were optimized for the deposition of stoichiometric $Ge_2Sb_2Te_5$ films. During each precursor purge step, Ar gas was introduced at a flow rate of 200 sccm (standard cubic centimeter per min) for 2−4 s. The sequence of the precursor pulses was Sb−Te−Ge−Te− (one supercycle was composed of four elemental cycles, where each elemental cycle consisted of a precursor and reactant injection followed by purge steps), as determined in a previous study.[4] After each precursor pulse and purge, Ar (200 sccm) + H_2 (200 sccm) reduction gas was pulsed for 2 s. During the entire precursor and reduction gas pulse period, radio frequency direct plasma was applied (rf power of 100 W) to the reaction chamber. After the reduction gas pulse period, another purge step using Ar gas (Ar purge) without plasma power was added for 6 s to completely remove the residual precursor and reduction gases. Under these growth conditions, a typical growth rate (thickness per supercycle) was ∼0.4 nm cycle^{-1}.

The types of substrates investigated were SiO_2, Si_3N_4, TiO_2, ZrO_2, HfO_2, and TiN layers. SiO_2 and Si_3N_4 films were deposited on a Si substrate by chemical vapor deposition, while TiO_2, ZrO_2, and HfO_2 films were deposited on the chemical vapor deposited SiO_2 layer by atomic layer deposition. The TiN films were deposited on a SiO_2 substrate by sputtering. The reason for the selection of these substrates is as follows. For fabricating the conventional T-shaped and contact-plug confined PcRAM cells, GST thin films should be homogeneously and evenly deposited on both the metallic contact plug surface and interlayer dielectric, which usually consists of CVD SiO_2 and Si_3N_4, where the metal plugs are embedded. The contact plug is usually TiN. However, as shown in this report, the growth behavior of GST film on the metallic TiN and insulating SiO_2 (Si_3N_4) surfaces is very different. Therefore, conformal atomic layer deposited buffer layers are necessary as a seed layer to form a uniform GST film. ALD TiO_2, ZrO_2, and HfO_2 thin layers are tested as a seed layer because they can be uniformly deposited on the complicated structure. Furthermore, the uniformly grown very thin oxide layer (<5 nm) could work as a heat insulation layer that improves the PcRAM performance without serious intervening contact resistance effect.[6]

The growth behavior, chemical composition, and areal layer density of the film were examined using an X-ray fluorescence analyzer (XRF, TN spectra QuanX), for which the atomic concentration and density measurements were calibrated by proton-induced X-ray emission (PIXE, Canberra 12170). The cross section of the film was examined by field-emission scanning electron microscopy (FESEM, Hitachi S-4800) and high resolution transmission electron microscopy (HRTEM, JEOL JEM-3000F). The surface morphology was investigated by atomic force microscopy (AFM, JEOL JSPM-5200) and FESEM. The crystal structure of the film was analyzed by X-ray diffraction (XRD, PANalytical X-pert Pro) in $\theta-2\theta$ and glancing angle mode (GAXRD, incidence angle 1°). The chemical binding state of the GST film and interfacial layer between the GST and the substrate were examined by X-ray photoelectron spectroscopy (XPS, ThermoVG Sigma Probe) using Al Kα X-rays.

III. Results and Discussions

III-1. Film Growth Behaviors. Figure 1a shows the variations in the film layer density on the various substrates as a function of the number of supercycles (n_{cy}). The substrates could be divided into three groups according to the growth behavior of the GST film. TiN and TiO_2 were higher-growth substrates (HGS); SiO_2, Si_3N_4, and ZrO_2 substrates were lower-growth substrate (LGS); and HfO_2 was a nongrowth substrate (NGS) where virtually no film growth was observed. There was certain number of n_{cy}, where the GST film did not grow on the LGS. The number of incubation cycles (n_{cy}^{i}) was typically 20−25 cycles. The presence of n_{cy}^{i} was usually attributed to the poor nucleation of the growing films. Therefore, the nucleation of GST films on a LGS is less favorable than on a HGS. The complete nongrowth of GST on the HfO_2 surface suggests that the precursors never adsorb to this substrate. Interestingly, a comparison of the growth behavior of GST film on the HGS and LGS showed that the saturated growth rates (G_{sat}, which is slope of the graphs shown in Figure 1a) were different on the HGS and LGS. Once the substrate was covered with the growing GST film, further growth was just a repeat of the growth process on the same GST material. Therefore, the G_{sat} should be independent of the types of the substrates if the growing films are identical. Therefore, the films grown on the HGS and LGS substrates are in some way different, as can be understood from the discussions shown in section III-3.

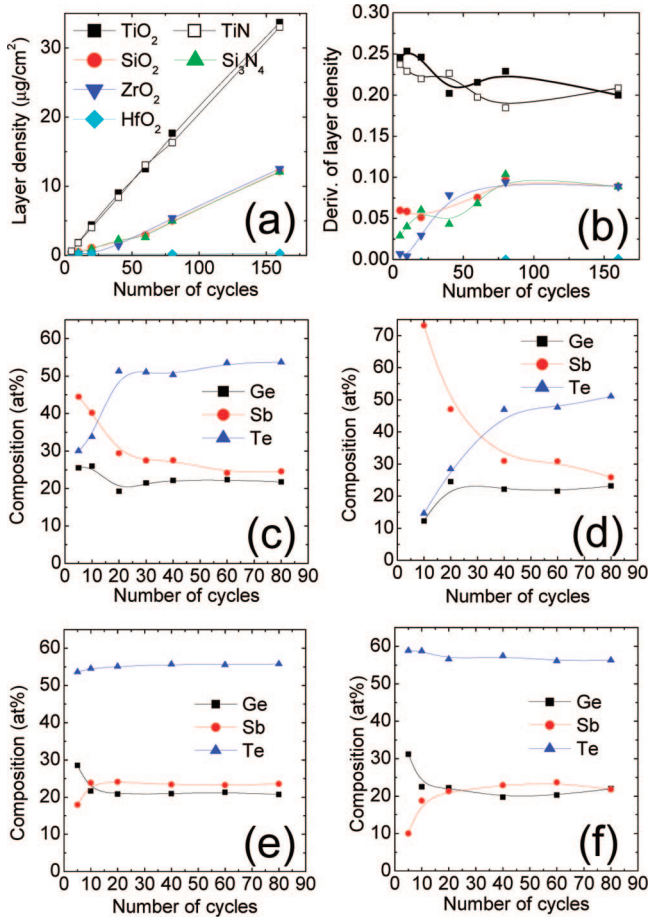

Figure 1. (a) Changes in film layer density on the various substrates as a function of the number of supercycles (n_{cy}), (b) derivative of the layer density in (a) as a function of n_{cy}, and (c−f) the variations in the film composition on SiO_2, Si_3N_4, TiO_2, and TiN substrates, respectively as a function of n_{cy}. The substrates could be divided into three groups according to the growth behavior of the GST film. TiN and TiO_2 were HGSs; SiO_2, Si_3N_4, and ZrO_2 substrates were LGSS; and HfO_2 was a NGS. The film growth was generally more uniform on TiO_2 and TiN.

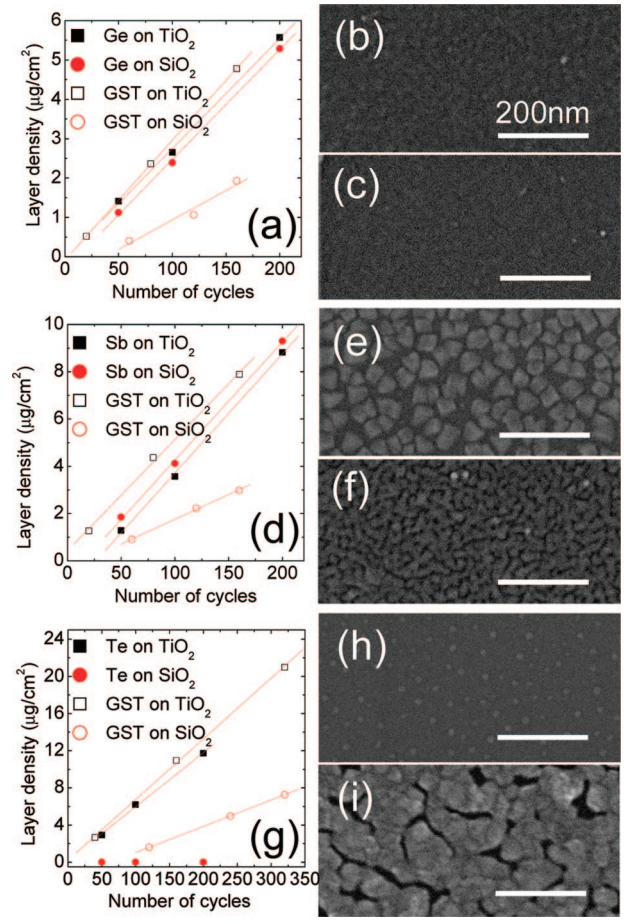

Figure 2. Changes in elemental (a) Ge, (d) Sb, and (g) Te layer density, respectively, of the films deposited on the TiO_2 and SiO_2 substrates as a function of n_{cy} and SEM images of the (b, c) elemental Ge films (100 cycles), (e, f) Sb films (100 cycles), and (h, i) Te films (100 cycles) on the (b, e, h) SiO_2 and (c, f, i) TiO_2 substrates. It appears that elemental Ge and Sb film growth does not show serious substrate dependency, but the GST film shows very severe substrate dependency.

Figure 1b shows the derivative of the layer density in Figure 1a as a function of n_{cy}, which corresponds to the growth rate at each n_{cy}. The derivatives were initially higher but decreased with increasing n_{cy} and then saturated on the HGS. However, on the LGS, they increased with increasing n_{cy} and saturated at a value lower than on the HGS. The higher growth rate at the early stage shows that the nuclei were easily formed on the HGS surface, whereas the lower growth rate indicates retarded nucleation properties on the LGS and NGS surfaces.[13]

Figure 1c−f show the changes in the film composition on SiO_2, Si_3N_4, TiO_2, and TiN substrates, respectively, as a function of the n_{cy}. On LGSs (SiO_2 and Si_3N_4), the film composition was not uniform but dependent on n_{cy}. A Sb-rich and Te-deficient film initially formed, and then the Te concentration increased to 50−55% after 20−40 cycles. However, the film growth was generally more uniform on the HGS (TiO_2 and TiN). A slightly Ge-rich and Sb-deficient film was deposited on the HGS in the initial growth stage (n_{cy} < ∼10 cycles), but a stoichiometric film was soon obtained above 10 cycles.

To understand the nucleation and growth behavior of each component on the different types of substrate, elemental Ge, Sb, and Te films were deposited on TiO_2 (a typical HGS) and SiO_2 (a typical LGS), and the results were compared with the cases of GST film deposition on the same substrates. Figure 2a,d,g shows the variations in the elemental Ge, Sb, and Te layer density of the films on the TiO_2 and SiO_2 substrates as a function of n_{cy}. The incorporation behavior of the same elements into the GST film is also shown for comparison. Here, for the GST film, only the number of Ge, Sb, and Te subcycles are counted in parts a, d, and g, respectively. Because two Te subcycles were included in a single supercycle, the number of Te cycles in part g was double that in parts a and d. The Ge film showed a similar saturated growth rate on both TiO_2 and SiO_2 substrates (same slope) but slightly longer incubation cycles on SiO_2 than on TiO_2. Figure 2 b,c shows SEM surface micrographs of the elemental Ge films (100 cycles) grown on the SiO_2 and TiO_2 substrates. A uniform and dense microstructure was observed on both substrates. The rate of Ge incorporation into the GST on the TiO_2 substrate was almost identical to that of the elemental Ge film. However, it was much lower on the SiO_2 substrate, showing an n_{cy}^{i} of ∼30 cycles and almost half the G_{sat} than others in the GST film.

(13) Puurunen, R. L. *J. Appl. Phys.* **2005**, *97*, 121301.

Elemental Sb film also has a similar G_{sat} on both TiO_2 and SiO_2 substrates (same slope), but its n_{cy}^i was generally non-negligible. n_{cy}^i was slightly longer on TiO_2 than on SiO_2, which is in contrast to the Ge case. Figure 2e,f shows SEM surface micrographs of the elemental Sb films (100 cycles) on the SiO_2 and TiO_2 substrates. Because of the non-negligible n_{cy}^i in this case, the films were not continuous but contained a large number of voids. The Sb film on the SiO_2 substrate appears to have a lower nucleation density but a larger average grain size. Interestingly, there was more enhanced Sb incorporation in the GST film on the TiO_2 substrate than elemental Sb deposition. There was no n_{cy}^i, which corresponds to a previous report, where the self-catalytic growth behavior of GST was observed.[5] However, the incorporation of Sb into the GST film on the SiO_2 substrate was largely hindered also.

The elemental Te film growth behaviors showed an extreme substrate dependent behavior (Figure 2g). Although the rate of elemental Te growth on the TiO_2 substrate is quite fluent and almost identical to the rate of Te incorporation into the GST on the same substrate, elemental Te never grew on the SiO_2 substrate. The incorporation of Te into the GST on SiO_2 is possible by a self-catalytic effect but is significantly lower than on TiO_2. Figure 2h,i shows SEM surface micrographs of the elemental Te films (100 cycles) on the SiO_2 and TiO_2 substrates. Only very small nuclei were observed on the SiO_2, of which the amount is too small to be detected by XRF. However, the Te film reasonably grew well on the TiO_2 substrate. The presence of many intergranular voids suggests that the nucleation density was not high enough to ensure dense and uniform Te film growth, even on the TiO_2 surface.

It appears that elemental Ge and Sb film growth does not show serious substrate dependency, but the GST film shows very severe substrate dependency. This discrepancy was attributed to the different in situ crystallization behavior, which was caused by the different nucleation and impurity diffusion behaviors of the GST film on the different types of substrates and the different Te incorporation on the different substrates as shown in sections III-2 and III-3.

These results coincide well with the changes in GST film composition with n_{cy}, as shown in Figure 1. The initially high (low) concentration of Ge (Sb) on the HGS is related to the different n_{cy}^i of the Ge and Sb deposition on these substrates. The inverse trend of the initial Ge and Sb incorporation on the LGS could also be attributed to the same reason.

Parts a−c and d−f of Figure 3 show the SEM surface morphology and the cross section of the GST films grown on SiO_2, TiO_2, and TiN substrates, respectively. Here, n_{cy} values of the GST films were controlled to 160 on SiO_2 and 80 on TiO_2 and TiN to achieve a similar film thickness. The GST film on the SiO_2 layer shown in Figure 3a had a rough surface, larger average grain size, and island-type growth behavior compared to the GST film on other substrates. On the other hand, the GST films on the TiO_2 and TiN layers show a high nucleation density, very smooth surface, and layer-type growth behavior.

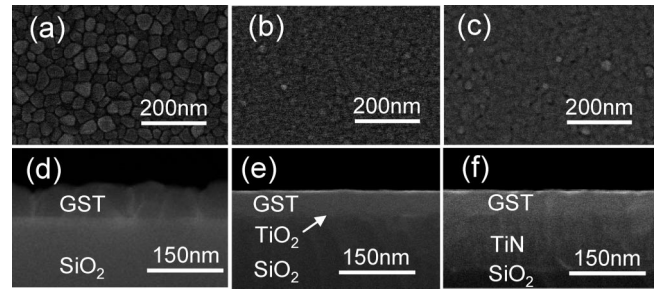

Figure 3. SEM images of (a−c) surface morphology and (d−f) cross section of the GST films grown on SiO_2, TiO_2, and TiN substrates, respectively. To achieve a similar film thickness, the n_{cy} of the GST films was 160 on SiO_2 and 80 on the TiO_2 and TiN substrates.

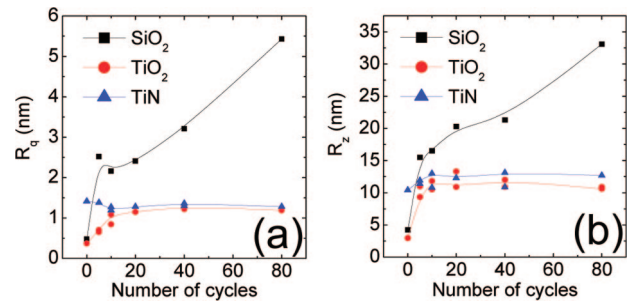

Figure 4. Changes in (a) the rms roughness (R_q) and (b) 10-point median roughness (R_z), obtained by AFM of the GST films on the SiO_2, TiO_2, and TiN substrates as a function of n_{cy}.

Figure 4a,b shows the changes in the root-mean-squared (rms) roughness (R_q) and 10-point median roughness (R_z), by AFM of the GST films on the SiO_2, TiO_2, and TiN substrates as a function of n_{cy}. R_q was slightly lower on the TiO_2 layer until 10 cycles and saturated to ∼1.2 nm. It was ∼1.3 nm on TiN layer irrespective of n_{cy}. This was attributed to the smoother surface of ALD TiO_2 compared to the sputter-deposited TiN. The R_q of the GST films on the SiO_2 layer became much rougher with increasing n_{cy}. R_z shows similar tendencies to R_q on the various substrates. These results are consistent with the variations in the nucleation behavior shown above.

The crystal structure of the GST films was examined by XRD and HRTEM. Figure 5 a,b shows the XRD patterns of the GST film grown on SiO_2, TiO_2, and TiN substrates measured in the $\theta-2\theta$ and glancing angle mode, respectively. n_{cy} values of GST were 160 on SiO_2 and 80 on TiO_2 and TiN. The GST film on SiO_2 did not show any distinct diffraction peaks in $\theta-2\theta$ mode but showed weak fcc (111) and (220) peaks for GST in glancing angle mode, suggesting that the GST grew with a weakly crystallized phase or very fine grain size on the SiO_2 surface. This is apparently in contradiction to the SEM observations shown in Figure 3, where a larger grain size was observed. This suggests that the granular shaped materials in Figure 3a are not crystallized GST grains. This was actually confirmed by HRTEM, as shown in Figure 6. However, the GST films on the TiO_2 and TiN substrates clearly showed fcc (200) and (220) peaks in both $\theta-2\theta$ and glancing angle modes. The similar relative peak intensities in the $\theta-2\theta$ and glancing angle modes suggests that the preferred growth behavior was weak. All these GST films contained a much lower carbon impurity concentration.[4]

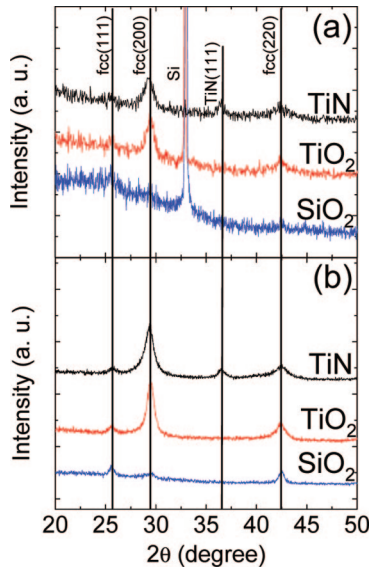

Figure 5. XRD patterns of the GST film grown on SiO_2, TiO_2, and TiN substrates measured in (a) the $\theta-2\theta$ and (b) glancing angle mode. n_{cy} of GST were 160 on SiO_2 and 80 on TiO_2 and TiN. The GST films on the TiO_2 and TiN substrates clearly showed fcc (200) and (220) peaks in both $\theta-2\theta$ and glancing angle modes. The GST film on SiO_2 showed weak fcc (111) and (220) peaks for GST in the glancing angle mode, suggesting that the GST grew with a weakly crystallized phase or very fine grain size on the SiO_2 surface.

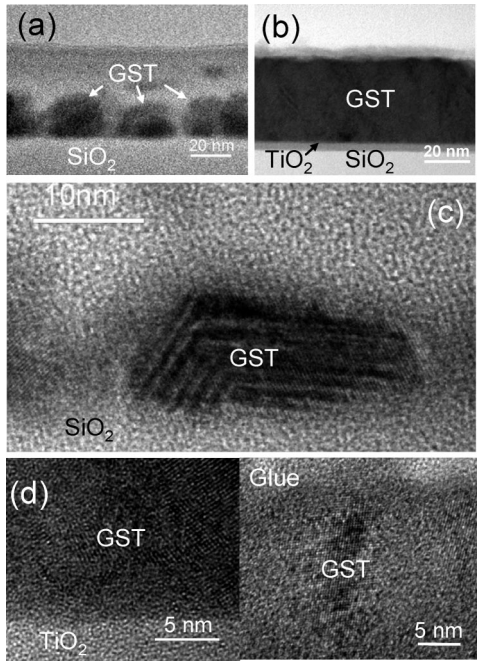

Figure 6. Low magnification cross section TEM images of a GST film (80 cycles) on (a) SiO_2 and (b) TiO_2 substrates. HRTEM images of a GST island on (c) SiO_2 and (d) the interface (left) and top surface regions (right) of GST film on a TiO_2 substrate. The GST island on SiO_2 had a single fcc crystalline structure inside the islands with an amorphous material surrounding it, which suggested that the initial nuclei might be amorphous but that they transform to a crystalline material with increasing deposition time due to the temperature effect. The GST films on the TiO_2 layer consisted of a densely packed number of small polycrystalline columnar grains.

Figure 6a,b shows low magnification cross section TEM images of the GST film on SiO_2 and TiO_2 substrates. Here, the growth cycles were both 80, respectively. GST islands with a hemispherical shape and a lower density formed on the SiO_2 layer, while a much smoother and densely packed film was observed on the TiO_2 layer. An in-depth investigation using HRTEM, shown in Figure 6c, shows that the GST island on SiO_2 had a single fcc crystalline structure (confirmed by the Fourier transformed diffraction patterns, data not shown) inside the islands with an amorphous material surrounding it. The space between the crystalline materials was sparsely filled with amorphous material. This morphology suggests that the initial nuclei might be amorphous, but they transform to a crystalline material with increasing deposition time due to the temperature effect. However, the atoms adhering to the GST surface are still amorphous so that the resulting microstructure has the appearance of that shown in Figure 6c. The GST films on the TiO_2 layer consisted of a densely packed number of small polycrystalline columnar grains, as shown in Figure 6d. The left and right panels of Figure 6d show HRTEM images of the interface and top surface regions, respectively. There was minimal incorporation of amorphous material on the top surface. The top surface region may contain some amorphous materials, but extensive TEM observation showed that it is mostly crystalline. Nucleation with a stoichiometric 2 (Ge):2 (Sb):5 (Te) composition in the early deposition stage on the HGS induced rapid crystallization because the growth temperature is approximately equal to the crystallization temperature of stoichiometric GST. However, nucleation with a Te-deficient nonstoichiometric composition on the LGS resulted in delayed crystallization due to the higher crystallization temperature of the Te-deficient material.[14] This difference in nucleation and resulting growth behaviors has a close relationship with the chemical interaction between the growing nuclei and substrates, as shown in section III-2.

III-2. Nucleation of GST Films. The GST thin films in the nucleation regime were examined by XPS to determine the chemical interactions between the GST film and substrates. Ar^+ ion sputtering with an acceleration voltage of 2 kV and a duration of 5 s was carried out prior to XPS analysis to remove the native oxide layer on the surface. The binding energy (BE) scale was calibrated using the C 1s binding energy at 284.8 eV. Figure 7a−c shows the XPS spectra of the Ge 2p, Sb 3d, and Te 3d core levels, respectively, of the GST thin film (seven cycles) on the SiO_2 substrate. The BEs of the Ge $2p_{3/2}$, Sb $3d_{5/2}$, and Te $3d_{5/2}$ peaks were observed at 1218.5, 528.7, and 572.6 eV. The reported BE positions of elemental Ge $2p_{3/2}$, Sb $3d_{5/2}$, and Te $3d_{5/2}$ core levels are 1217.2, 528.2, and 573.0 eV suggesting that the chemical shifts of the BE of Ge 2p, Sb 3d, and Te 3d were +1.3, +0.5, and −0.4 eV, respectively.[15,16] The BE of Te $3d_{5/2}$ in a GeTe alloy was reported to be 572.7 eV, which is comparable to that in this GST film.[15] Interestingly, the oxidation states of Ge (peak at 1220.1 eV) and Sb (peak at 531.1 eV) were observed. The peak at 1220.1 eV reasonably

(14) Wuttig, M.; Sebrinki, D. L.; Wamwangi, D.; Wełnic, W.; Gillessen, M.; Dronskowski, R. *Nat. Mater.* **2007**, *6*, 122.
(15) NIST Standard Reference Database 20, Version 3.4; Wagner, C. D., Naumkin, A. V., Kraut-Vass, A., Allison, J. W., Powell, C. J., Rumble, J. R., Jr., Eds. http://srdata.nist.gov/xps/ (2003).
(16) Jung, M.-C.; Shin, H. J.; Kim, K.; Noh, J. S.; Chung, J. *Appl. Phys. Lett.* **2006**, *89*, 043503.

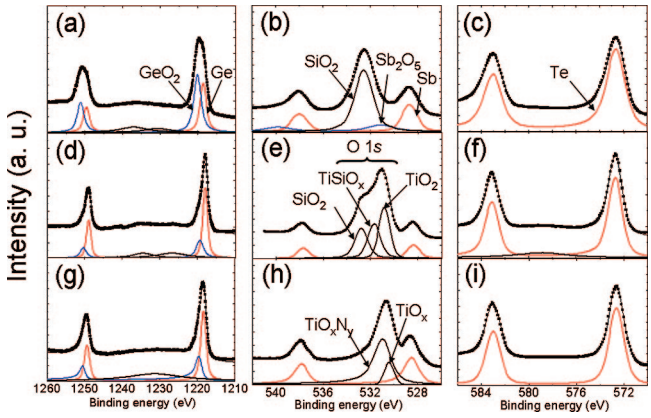

Figure 7. XPS spectra of the Ge 2p, Sb 3d, and Te 3d binding energies, respectively, of the GST thin film (seven cycles) deposited on (a−c) SiO_2, (d−f) TiO_2, and (g−i) TiN substrates. The oxidation states of GeO_2 (peak at 1220.1 eV) and Sb_2O_5 (peak at 531.1 eV) suggest that a significant portion of the adsorbed Ge and Sb atoms were oxidized, possibly by the oxygen supplied from the SiO_2 substrate. A GeO_2 was also detected on the TiO_2 and TiN substrate, but its relative intensity was much lower than the case of GST on the SiO_2. Sb was not oxidized on TiO_2 and TiN. A chemical interaction with oxygen was not found in Te in all cases.

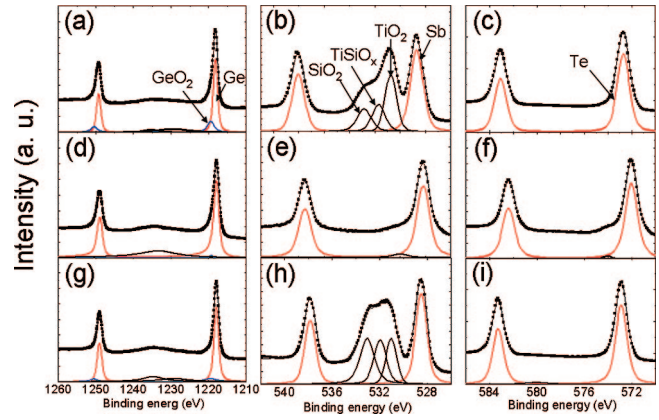

Figure 8. XPS spectra of the Ge 2p, Sb 3d, and Te 3d of GST thin films deposited on a TiO_2 substrate with n_{cy} = (a−c) 10 and (d−f) 60, respectively, followed by Ar^+ sputter-etching for 5 s. (g−h) n_{cy} = 60 followed by Ar^+ sputter-etching for 30 s. There was no notable change in the positions and shapes of the peaks from the alloy phase, suggesting that GST growth on TiO_2 occurred under steady state conditions. The oxidation of Ge was highly localized to the interface region, and oxygen diffusion into the bulk of the film was negligible even for a larger n_{cy}, at least up to 60.

matches the 4+ oxidation state of Ge in GeO_2 (peak at 1220.4 eV). Moreover, this peak intensity is slightly higher than that of the Ge $2p_{3/2}$ in the GST alloy phase. This suggests that a significant portion of the adsorbed Ge atoms were oxidized, possibly by the oxygen supplied from the substrate. The BE of 531.1 eV of Sb oxide was well matched that of Sb^{5+} in Sb_2O_5 (531.1 eV).[15] There is some overlap between O 1s from SiO_2 and the oxidation state of Sb, but the broadening of the Sb $3d_{3/2}$ peak near 540 eV can be explained by the presence of an Sb_2O_5 phase. In the case of Te, there was no chemical interaction with oxygen.

Parts d−f and g−i of Figure 7 show the XPS spectra of the Ge 2p, Sb 3d and Te 3d of the GST thin film (n_{cy} of seven cycles) on the TiO_2 and TiN substrates, respectively. The BEs of the Ge $2p_{3/2}$, Sb $3d_{5/2}$ and Te $3d_{5/2}$ peaks were 1218.0 (1218.3) eV, 528.4 (528.5) eV, and 572.7 (572.6) eV for the GST film on TiO_2 (TiN). These values are similar to those on the SiO_2 layer. A feature for oxidized Ge was also detected at 1219.4 (1219.5) eV on the TiO_2 (TiN) substrate, but its relative intensity compared with the peak from the GST alloy was much lower than the case of GST on the SiO_2. Although a clear estimation of the involvement of the Sb oxide is not possible because of the presence of O 1s peaks from SiO_2, $TiSiO_x$, and TiO_2 from 530 to 534 eV, the absence of a broad shoulder near the BE of 540 eV suggests that Sb was not oxidized in these cases. The presence of a SiO_2 peak was attributed to the very thin (∼2 nm) TiO_2 grown on the SiO_2 substrate. It is well-known that the surface of TiN usually contains TiO_x because of oxidation so that the O 1s peaks from TiO_xN_y and TiO_x are observed in Figure 7h.[22] This is actually one of the reasons for the similar growth behavior of GST on the TiO_2 and TiN substrates. A chemical interaction with oxygen was not found in Te in these cases too.

XPS of the thicker GST films on TiO_2 were also carried out to examine the evolution of the chemical interaction with the increasing film thickness. Parts a−c and d−f Figure 8 show the XPS spectra of the Ge 2p, Sb 3d, and Te 3d of GST thin films on the TiO_2 substrate deposited with the n_{cy} of 10 and 60, respectively, followed by Ar^+ sputter-etching for 5 s. As n_{cy} increased, the peak intensities from the GST alloy increased with a concomitant decrease in the peaks from the underlying layers and GeO_2. There was no notable change in the positions and shapes of the peaks from the alloy phase suggesting that GST growth on TiO_2 occurred under steady state conditions. For the film deposited with 60 cycles, only peaks from the alloy phase were observed suggesting a chemically pure structure of the thin films. Figure 8g−h shows the same XPS spectra of the film deposited with the n_{cy} of 60 followed by Ar^+ sputter-etching for 30 s. From a comparison of the peak intensities, the remaining film thickness was ∼10 nm. Although the relative chemical composition of the surface was largely altered by the severe etching, there were no notable peaks corresponding to the GeO_2 and Sb_2O_5. This suggests that the oxidation of Ge was highly localized to the interface region, and oxygen diffusion into the bulk of the film was negligible even for a larger n_{cy}, at least up to 60. However, this was not the case for the GST film deposited on the SiO_2 substrate. The emergence of O 1s (BE from ∼530 to 534 eV) peaks from the substrate layers even with such a thick nominal thickness of the GST film might be due to the nonuniform etching of GST.

Figure 9a−c shows the Ge 2p, Sb 3d, and Te 3d XPS spectra of the GST film deposited on the SiO_2 substrate with n_{cy} = 5 followed by the Ar^+ sputter-etching for 5 s, and Figure 9d−f shows the corresponding peaks of the film deposited with n_{cy} = 60 followed by Ar^+ sputter-etching for 30 s. In these cases, oxidation was so serious that oxide peaks for Ge and Sb were always detected. This suggests that a part of the SiO_2 substrate is reduced, which supplies the GST material with oxygen. When the film becomes thicker, the chemical interaction between the film and the substrate becomes even more serious so that the oxidation states of Ge and Sb become quite complicated, as shown in Figure 9d,e. In this case, some of the Te was also oxidized, even though the concentration of the

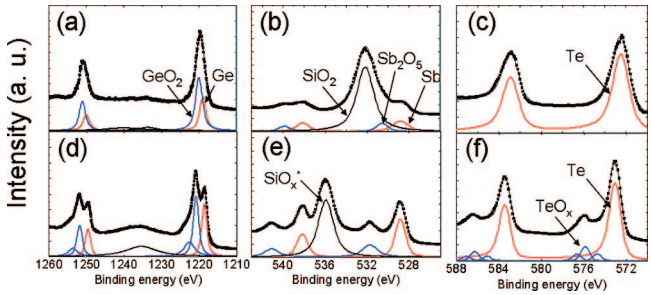

Figure 9. Ge 2p, Sb 3d, and Te 3d XPS spectra of the GST film deposited on the SiO_2 substrate with the (a−c) $n_{cy} = 5$ followed by Ar^+ sputter-etching for 5 s and (d−f) the $n_{cy} = 60$ followed by Ar^+ sputter-etching for 30 s. Oxidation was so serious that oxide peaks for Ge and Sb were always detected, suggesting that a part of the SiO_2 substrate is reduced, which supplies the GST material with oxygen. Partial charging effect may shift the BE of the O 1s peak abnormally into the higher binding energy due to excessive sputter-etching and low conductivity of GST film on the SiO_2 substrate.

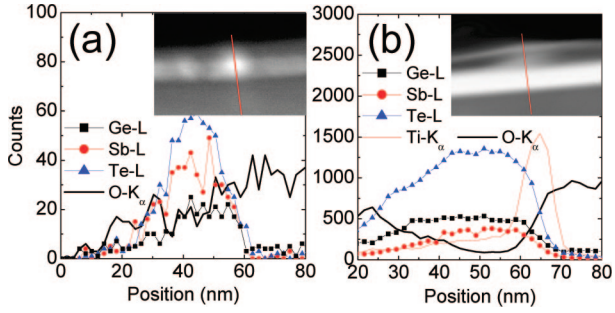

Figure 10. EDS scan results along the lines shown in the inset scanning TEM images of the GST film on the (a) SiO_2 and (b) TiO_2, respectively, substrates. The diffusion of oxygen from SiO_2 into the GST film was much more severe than the case of GST on TiO_2. This may have a close relationship with the suppressed crystallization of GST on the SiO_2 substrate.

oxidized Te was relatively low. The BE of the O 1s peak shifted abnormally into the high binding energy (indicated by the arrow in Figure 9e), which could not be assigned to any oxides of the component materials. Partial charging effect may shift the peak position into the higher binding energy because of excessive sputter-etching and low conductivity of the GST film on the SiO_2 substrate. Although the clear identification of all these XPS spectra was not possible, it is quite clear that there was significant chemical interaction and interdiffusion between the GST film and the SiO_2 substrate. This may interfere adversely with the crystallization of the nuclei, as shown in Figures 5 and 6. XPS of the thicker GST film on SiO_2 (spectra from the film deposited with the $n_{cy} = 60$ followed by Ar^+ sputter-etching only for 5 s) did not show any distinctive features from that shown in Figure 8 d−f, suggesting that the chemical interaction was limited to the thinner part of the film close to the substrate. This coincides with the change in chemical composition with the film thickness shown in Figure 1c.

This was further confirmed by energy dispersive spectroscopy (EDS) of the samples shown in Figure 6. Figure 10a,b shows the EDS results along the lines shown in the inset scanning TEM images of the GST film on SiO_2 and TiO_2, respectively. Although the oxygen signal was always detected as a result of the partial oxidation of the TEM

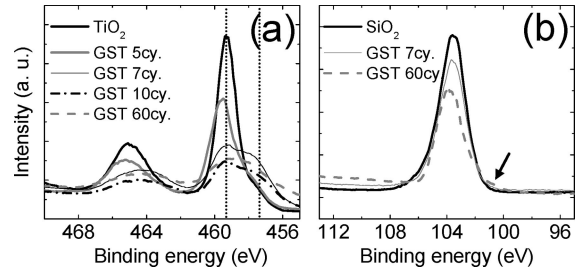

Figure 11. XPS spectra of (a) the Ti 2p of the TiO_2 substrate when the GST film of $n_{cy} = 5$, 7, 10, and 60 cycles, (b) Si 2p of SiO_2 substrate when GST film of n_{cy} of 7, and 60 cycles were grown on it. The TiO_2 surface is heavily reduced during the GST deposition. The Si 2p spectra show no notable change in shape except for the overall decrease in intensity when the GST film was deposited.

specimen surface, it was clearly observed that the diffusion of oxygen from SiO_2 into the GST film was much more severe than the case of GST on TiO_2. This may have a close relationship with the suppressed crystallization of GST on the SiO_2 substrate. The changes in the chemical states of the TiO_2 and SiO_2 layers are also investigated by the XPS.

Figure 11a shows the XPS spectra of the Ti 2p of the TiO_2 substrate with a GST film deposited at $n_{cy} = 5$, 7, 10, and 60 cycles. For the thick GST film case ($n_{cy} = 60$), the film was etched back by Ar^+ ion sputtering to probe the TiO_2 surface. The figure also contains the XPS spectra of the TiO_2 substrate itself before film deposition for comparison. Although the Ti $2p_{3/2}$ peak of the 2-nm-thick TiO_2 thin film on SiO_2 was shifted slightly from the binding energy of stoichiometric TiO_2 (459.5 eV), it consists mainly of a single component corresponding to TiO_2. However, once the GST films are deposited, even after only five cycles, a peak with a lower BE emerged, which was similar to the BE of Ti_2O_3 (457.8 eV).[17] The intensity of this lower BE peak appears to be comparable to that of TiO_2 suggesting that the TiO_2 substrate was heavily reduced by GST deposition. This has a close relationship with the fluent nucleation of GST on the TiO_2 substrate. As a result of the limited oxygen supply from the very thin TiO_2 layer, the oxidation of the GST nuclei was limited to only Ge, which has the highest oxidation potential among Ge, Sb, and Te.

The changes in the Si 2p XPS spectra from the SiO_2 substrate were also examined when the GST film was deposited (Figure 11b). The XPS spectra of the SiO_2 substrate itself (thicker line) consisted exclusively of Si^{4+} with a negligible contribution from the suboxides. When the GST film was deposited by seven cycles, the Si 2p spectra show no notable change in shape except for the overall decrease in intensity. This is interesting considering the much more extensive oxide formation of Ge and Sb and higher oxygen concentration in the GST film on this substrate. This apparent contradiction can be resolved by assuming that the SiO_x ($x \ll 2$) formed was removed from the surface by volatilization. Although the substrate temperature (150 °C) was too low to induce such volatilization, it should be noted that the system is under the plasma bombardment conditions, which

(17) Aizawa, M.; Lee, S.; Anderson, S. L. *J. Chem. Phys.* **2002**, *117*, 5001.

may etch the SiO_2.[18,19] Evidence for this assumption can be found from the Si 2p XPS spectra from the GST film deposited by 60 cycles followed by Ar^+ sputtering. Since the remaining film thickness was slightly lower than ~10 nm (note that the initial thickness of this film was lower than that on TiO_2 even with the same n_{cy} due to the longer n_{cy}^i on SiO_2), the Si 2p peak has a contribution from both the SiO_2 substrate and possibly the SiO_x incorporated in the GST film. The presence of a distinct shoulder in the lower BE suggests that the incorporated SiO_x is oxygen deficient. Unfortunately, confirmation of the presence of SiO_x in the GST film using scanning TEM-EDS was not feasible due to the heavy contribution of the spurious X-ray from Si substrate to the EDS signal. The adverse interference from the SiO_2 substrate retards the formation of a stoichiometric GST film during the initial stages of film growth, as shown in Figure 1. The preferential oxidation of Ge and Sb due to its higher oxidation potential than Te results in a highly Te-deficient concentration on the SiO_2 substrate during the initial stages of film growth. As the film became thicker, the adverse interference from the SiO_2 substrate decreased and the film composition became similar to the stoichiometric value.

The above observations can explain the substrate dependent crystallization behavior of the GST films, as shown below. Oxide substrates usually contain surface functional hydroxyl groups with a density that depends strongly on the nature of the oxide itself and the experimental conditions.[20] An interaction between the surface hydroxyl group and ligand can induce the chemical adsorption of precursor molecules. These adsorbed precursor molecules undergo a surface reaction with the incoming reactant gas with subsequent nucleation. Concerning the M_xO_y oxides, the ionic character plays a key role because their acidic or basic properties can influence the density of surface functional groups. In addition, M^+ acidic Lewis sites or MO^- basic sites can themselves interact with the precursor ligand resulting in the adsorption of precursor molecules on these reactive sites.[20] The effects of ionic or metallically bonded substrates can also be explained by facilitation of a surface reaction due to the donation of electrons from the surface to the adsorbed molecules compared to the covalently bonded substrates.[21,22] However, there is no general rule for predicting what type of surface chemistry will be afforded in a given system. Therefore, the chemical interaction between each precursor molecule and substrate material could be quite complicated.[20]

In this experiment, the chemical adsorption of precursor molecules on the acidic or basic active sites of oxide substrates at such a low deposition temperature can be ruled out because of the stable alkyl ligands of the Ge, Sb, and Te precursor molecules, even though they were activated by the plasma. If this chemical interaction is feasible, the complete nongrowth of elemental Te on SiO_2 and GST on HfO_2 would not be observed.

Table 1. Difference in Electronegativity and Diatomic Bond Enthalpy of the Substrate and GST Materials in the Gaseous State at 298 K[24]

	difference in electronegativity	diatomic bond enthalpy [kJ/mol]
Si−O	1.54	799.6 ± 13.4
Si−N	1.14	470 ± 15
Ti−O	1.9	672.4 ± 9.2
Ti−N	1.5	476.1 ± 33.1
Zr−O	2.11	776.1 ± 13.4
Hf−O	2.14	801.7 ± 13.4
Ge−O	1.43	659.4 ± 12.6
Sb−O	1.39	434.3 ± 41.8
Te−O	1.34	376.1 ± 20.9

In CVD of metal films, such as Al[11,12] and Ru,[21,22] the higher ionic character of the substrate enhanced nucleation. However, in this experiment, the more ionic ZrO_2 and HfO_2 compared to TiO_2 showed lower or even nongrowth properties. Hence, the promotion of nucleation from the ionic bonding nature of the substrate cannot explain the experimental results.

The most feasible explanation for the substrate dependent growth behavior of the GST film is to consider electron donation from the substrate, which would enhance precursor decomposition and the removal of ligands from the adsorbed precursor molecules. Although all the substrates except for TiN were insulators, their surface states were heavily modified during GST deposition, probably due to the application of plasma power. As shown in Figure 11a, the TiO_2 surface is heavily reduced resulting in free electrons that could be donated to the adsorbed precursor molecules. This may enhance the nucleation of the thin films. Even without plasma power, the TiO_2 surface is usually oxygen deficient, which can enhance the nucleation of GST on TiO_2.[23] The comparable oxidation potential of GeO_2 to that of TiO_2 also enhances the reduction of TiO_2.

On the other hand, the reduced SiO_2 is easily removed by its volatilization (with the help of the plasma power) so that the substrate surface could remain insulating. This may not enhance the nucleation of GST on SiO_2. Table 1 shows the diatomic bond enthalpy of the substrate and GST materials at a gaseous state at 298 K.[24] The Ge−O bond enthalpy is comparable to that of the Ti−O bond, whereas Zr−O and Hf−O have higher diatomic bond enthalpies. This also explains the lower nucleation rate of GST on the ZrO_2 substrate as well as the nongrowth of GST on the HfO_2 substrate; that is, Ge cannot reduce them. The reduction of these materials by plasma was also suppressed due to their stronger bonding. Even if the plasma power partially reduced them, they may be preferably oxidized again over Ge and the other metallic component in the system.

Redox of the oxide surface and precursors has been observed on several CVD or ALD processes.[11,20,25−28] Al

(18) Hofmann, K.; Raider, S. I. *J. Electrochem. Soc.* **1987**, *134*, 240.
(19) Ouyang, M.; Yuan, C.; Muisener, R. J.; Boulares, A.; Koberstein, J. T. *Chem. Mater.* **2000**, *12*, 1591.
(20) Serp, P.; Hierso, J.-C.; Kalck, P. *Top. Organomet. Chem.* **2005**, *9*, 147.
(21) Kang, S. Y.; Hwang, C. S.; Kim, H. J. *J. Electrochem. Soc.* **2005**, *152*, C15.
(22) Kim, B. S.; Kang, S. Y.; Seo, H. S.; Hwang, C. S.; Kim, H. J. *Electrochem. Solid-State Lett.* **2007**, *10*, D113.
(23) Smyth, D. M. *The defect chemistry of metal oxides*; Oxford University Press: New York, 2000; p 218.
(24) Kerr, J. A. *CRC Handbook of Chemistry and Physics: A Ready-Reference Book of Chemical and Physical Data*, 81st ed.; CRC Press: Boca Raton, 2000.
(25) Simmonds, M. G.; Taupin, I.; Gladfelter, W. L. *Chem. Mater.* **1994**, *6*, 935.
(26) Imaduddin, S.; Lad, R. J. *Surf. Sci.* **1993**, *290*, 35.

atoms on TiO_2 lead to the formation of reduced Ti centers as well as aluminum oxide.[25,26] Ni_3Al forms when the NiO surfaces are exposed to Al atoms.[25,26] In addition, when the metal oxides are reduced by the precursors, they, or their reduced products, can catalyze the further growth of nuclei.[25] The reduction and removal of the surface oxides from GaAs and InGaAs substrates by ALD of Al_2O_3 and HfO_2 have been reported.[28] Therefore, the severe interaction of the substrate oxide layer with the growing materials and the possible reduction of them that eventually leads nucleation is not a peculiar process.

The formation of GeO_2 by the reduction of the TiO_2 surface plays a key role in the nucleation of GST. As shown in Figure 2b, the n_{cy}^{i} for Sb incorporation was decreased when the GST alloy film was deposited compared with the n_{cy}^{i} of the elemental Sb film. Although an elemental Te film could be deposited on a TiO_2 surface, its nucleation properties were improved significantly when Te was incorporated into the predeposited GST film. Accordingly, the nucleation density was increased due to formation of a GeO_2 phase. Moreover, the surface, being a reduced metal oxide, catalyzed the further growth of preformed nuclei.

This was even more clearly demonstrated from a comparison between the elemental Te film growth and Te incorporation into the GST on SiO_2 substrate, as shown in Figure 2g. Although Te cannot be grown on highly insulating SiO_2, it can be incorporated into the (Te-deficient) GST nuclei because GST is much more conducting than SiO_2. The relatively poor crystallization of the GST film on the SiO_2 substrate can be understood from the severe incorporation of oxide materials into the growing films.

III-3. Substrate Dependent Growth Kinetics of GST. It is usually expected that the substrate dependency of the growth rate disappears after surface reconstruction is masked by a thicker film.[11] However, instead of the substrate, the physical or crystallographic properties of the growing films, such as the electrical conductivity, surface morphology, crystallinity, and texture, can influence the film growth behavior even in the saturated growth region.[11,12,29−31] A higher growth rate is expected when the film has a rougher surface due to the larger surface area.[29] It should be noted that the crystallinity or texture of a film can impact the kinetic parameters, which are determined by surface reactions between the precursor molecules and surface active sites of the predeposited film.[12,30,31] In this section, the temperature dependence of the growth rate was examined from the viewpoint of kinetics, and the possible reasons for the different kinetic parameters of the GST film depending on the substrate type were investigated.

Figure 12a shows the change in the G_{sat} as a function of the inverse deposition temperature for GST deposition on TiO_2 substrate with the different pressure and plasma power

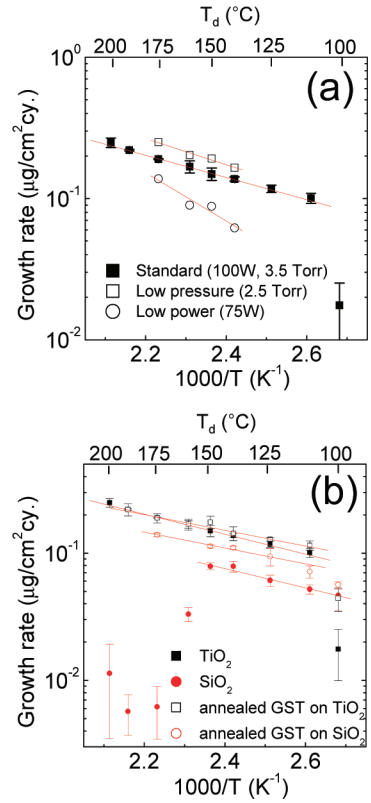

Figure 12. (a) Changes in the G_{sat} as a function of the inverse deposition temperature (1000/T) for GST deposition on TiO_2 substrate with the different pressure (□) and plasma power (○) conditions and (b) changes in the G_{sat} of the GST film on the TiO_2 (■), SiO_2 (●), and in situ annealed GST sublayers on TiO_2 (□) and SiO_2 (○) substrates, respectively. The activation energy for standard experimental conditions is 15.1 ± 0.8 kJ mol^{-1}, and this value is almost same irrespective of the substrate. However, the pre-exponential factor was largely dependent on the crystallization of the growing film surface. The crystallized GST surface decreased the activation energy for the chemisorption of the precursors and provided the growing film with the necessary charge exchange, which enhanced the saturated growth rate.

conditions. The dependence of the G_{sat} on the substrate temperature and source flux can be expressed as follows:[11,30,32,33]

$$G_{sat} = \sigma S^{R} k_0 \exp\left(-\frac{E_a}{RT}\right) = A \exp\left(-\frac{E_a}{RT}\right) \qquad (1)$$

where σ is the source flux, S^{R} is the reactive sticking probability, k_0 is the pre-exponential reaction constant, and A and E_a are the apparent frequency factor and activation energy for the reaction, respectively. This Arrhenius type equation describes the overall qualitative dependence of the growth rate on the relevant parameters and determines if diffusion-limited (transport-limited) or surface-reaction-limited deposition occurs from the estimated activation energy values.[11] The E_a for standard experimental conditions is 15.1 ± 0.8 kJ mol^{-1}, as determined from the slope of the line. This value is much lower than that previously reported for binary alloys using the DIPTe precursor, 100−150 kJ mol^{-1}.[32,34] This may suggest that deposition is proceeded by a diffusion-limited process. However, this was not the case

(27) Mantell, D. A. *J. Vac. Sci. Technol. A* **1991**, *9*, 1045.
(28) Hinkle, C. L.; Sonnet, A. M.; Voge, E. M.; McDonnell, S.; Hughes, G. J.; Milojevic, M.; Lee, B.; Aguirre-Tostado, F. S.; Choi, K. J.; Kim, H. C.; Kim, J.; Wallace, R. M. *Appl. Phys. Lett.* **2008**, *92*, 071901.
(29) Gates, S. M. *Chem. Rev.* **1996**, *96*, 1519.
(30) Bent, B. E.; Nuzzo, R. G.; Dubois, L. H. *J. Am. Chem. Soc.* **1989**, *111*, 1634.
(31) Chan, A. W. E.; Hoffmann, R. *J. Vac. Sci. Technol. A* **1991**, *9*, 1569.
(32) Wilkerson, K. J.; Kappers, M. J.; Hicks, R. F. *J. Phys. Chem. A* **1997**, *101*, 2451.
(33) Cooke, M. J.; Harris, G. *J. Vac. Sci. Technol. A* **1989**, *7*, 3217.
(34) McDaniel, A. H.; Wilkerson, K. J.; Hicks, R. G. *J. Phys. Chem. A* **1995**, *99*, 3574.

as shown below. The growth rate was increased when the total chamber pressure was decreased from 3.5 to 2.5 Torr with same partial pressure of the precursor, while E_a was maintained at a similar value, as shown in Figure 12a. This may result from the increased diffusion of the precursor molecules to the growing film surface, which increases σ in eq 1. On the other hand, when the plasma power applied during precursor feeding was decreased from 100 to 75 W, the growth rate was decreased and the E_a increased to 32.7 $\pm$ 6.0 kJ mol^{-1}. This suggests that the overall growth rate is influenced significantly by the surface chemical reaction rate rather than gas-phase diffusion. It is believed that the surface chemical reaction rate is increased largely by the assistance of the plasma power, which decreased the apparent E_a. Therefore, the E_a values estimated in this study represent the contribution of thermal energy to the proceeding of the chemical reactions.

The surface reaction mechanism in CVD of various tellurides using DIPTe has been studied extensively.[32,34,35] There are two most likely pathways, alkane recombination by radical reactions and olefin formation by disproportionation. It was reported that the radical reaction dominates disproportionation from the rate constant ratio. It could be understood that DIPTe is adsorbed dissociatively on the surface active sites forming radicals, and a radical reaction is enhanced by the high plasma power. Therefore, the activation energy for the radical reaction was reduced by the plasma power.

The changes in the G_{sat} of the GST film on the TiO_2 and SiO_2 substrates are also shown in the Arrhenius plot in Figure 12b. The estimated E_a for GST growth on the SiO_2 substrate (closed circles) was 14.6 $\pm$ 3.4 kJ mol^{-1}, which is similar to that on the TiO_2 substrate (closed squares). However, the absolute G_{sat} values were much smaller. Moreover, the absolute G_{sat} values decreased abruptly at temperatures > 160 °C. The smaller G_{sat} values at a temperature up to 150 °C suggest that the apparent frequency factor, A, is much smaller on the SiO_2 substrate. The abrupt decrease in G_{sat} value over 160 °C on the SiO_2 substrate may be due to the serious reduction of the SiO_2 substrate and severe volatilization of the SiO_x, which inhibits chemical adsorption of the precursors to the surface. This confirms the nucleation model proposed in section III-2. It is also possible that the partially decomposed DIPTe precursor is adsorbed on the substrate surface temporally, which inhibits the adsorption of the Ge and Sb precursors. Because Te cannot nucleate on SiO_2 at this temperature, this interference causes an abrupt decrease in growth rate. When these adverse reactions are not serious at temperatures < 160 °C, the lower G_{sat} value on the SiO_2 substrate can be understood from the reduced S^R because σ and k_0 should be the same. The S^R can be expressed as follows:[29,33,36]

$$S^R = \frac{1}{1 + \frac{k_c}{k_d}\exp[(E_c - E_d)/kT]} \quad (2)$$

where E_c and E_d are the activation energies for chemisorption and desorption, respectively, and k_c and k_d are the pre-exponential reaction constants for chemisorption and desorption, respectively. The adsorbed precursors can diffuse and chemisorb dissociatively on the surface or desorb from it. S^R decreases with increasing E_c, which is a barrier to chemisorption, and a S^R value on the order of 10^{-3} corresponds to the $(E_c - E_d)/kT$ of 7.[29,33] If the G_{sat} ratio between the TiO_2 and SiO_2 substrates is equal to the S^R ratio and S^R lies in a typical CVD range, <0.1, the S^R ratio can be written as follows:

$$\frac{S^R_{TiO_2}}{S^R_{SiO_2}} \cong \exp[\{(E_{c,SiO_2} - E_{c,TiO_2}) - (E_{d,SiO_2} - E_{d,TiO_2})\}/kT] = 2.15 \quad (3)$$

Here, the ratios of pre-exponential factors of S^R were assumed to be equal, and the ratio between the average G_{sat} of GST on the TiO_2 and SiO_2 substrates was 2.15 at temperatures ranging from 110 to 150 °C. A possible explanation for the difference in S^R values between the two substrates may be deduced from the different crystallinity as well as the resulting electrical conductivity of the film and impurity content. In the rock-salt (fcc) structure of GST, Te atoms occupy one octahedral site, whereas Ge and Sb atoms as well as vacancies randomly occupy the second octahedral lattice site. The atomic arrangements are similar to the close packed structure that provides a high density of chemical adsorption sites. This may enhance the G_{sat} on the TiO_2 substrate. However, on SiO_2, the GST film has a poorly crystallized structure and a relatively high impurity concentration. Therefore, adsorption of the precursor may not be so easy resulting in a reduced G_{sat}. In this case, it can be assumed that the E_d values are similar for both GST surfaces. Therefore, the difference between the E_c on SiO_2 and TiO_2 is ~0.028 eV (2.73 kJ mol^{-1}) at 150 °C. As the S^R values of CVD typically ranges from 0.1 to 0.001,[29,33,36] corresponding to an $(E_c - E_d)$ of 0.08−0.25 eV at 150 °C, this value is not a negligible portion of $(E_c - E_d)$. Hence, the lower E_c of the GST on TiO_2 surface plays a key role in achieving a high S^R.

There is another important parameter that influences the G_{sat} on the two substrates. Since the crystalline quality of the two growing GST films is largely different, the accompanying electrical conductivity is also different. The resistivity of the 30-nm-thick GST films on the TiO_2 substrate was ~75 mΩ cm, as measured by a 4-point probe. However, the GST film on the SiO_2 substrate with a similar thickness did not show a measurable sheet resistance, suggesting that the film was insulating. This may be related to the amorphous nature of the surface area and the intergranular region of this GST film, as shown in Figure 6c. As discussed in section III-2, the good electrical conductivity of the growing film surface is essential for the fluent growth of a GST film.

To confirm the effect of crystallization of the GST surface on the growth behavior, GST films were grown on the SiO_2 and TiO_2 substrates for 100 cycles at 150 °C and immediately annealed for crystallization at 200 °C in the growth reactor under an Ar atmosphere for 5 min. Additional GST films were then deposited on these annealed samples, and the growth behavior of the additional GST films was examined.

(35) Kappers, M. J.; Wilkerson, K. J.; Hicks, R. F. *J. Phys. Chem. A* **1997**, *101*, 4882.
(36) Coon, P. A.; Gupta, P.; Wise, M. L.; George, S. M. *J. Vac. Sci. Technol. A* **1992**, *10*, 324.

The open circle and square data points in Figure 12b correspond to the additional GST films on the annealed GST sublayers on the SiO_2 and TiO_2 substrates, respectively. Here, the layer density of the previously deposited GST was subtracted to show only the amount of GST deposited after in situ annealing. Indeed, in situ annealing of the GST sublayer on SiO_2 enhanced G_{sat}, because the sublayer was crystallized and became conducting. The resistivity of the annealed GST film on the SiO_2 was $\sim$5 Ω cm. Although the G_{sat} on the in situ annealed GST film on the SiO_2 substrate was still lower than that on the TiO_2 substrate, this enhancement clearly demonstrates the importance of the electrical conductivity and crystalline quality of the growing surface. The enhancement of G_{sat} for the TiO_2 substrate was negligible as the GST film on TiO_2 was already crystallized. In all cases, the E_a did not vary significantly.

IV. Conclusions

This study concerned the nucleation and growth behavior of the GST films by the combined PECVD/PEALD on various types of substrates. The substrates could be classified into three groups according to the nucleation and growth behavior of the GST film. The nucleation of the GST film on the SiO_2, Si_3N_4, and ZrO_2 substrates was seriously retarded compared to those on the TiN and TiO_2 substrates where fluent film growth was observed. There was no GST film growth on the HfO_2 substrate. The nucleation behavior also influenced the crystallization of the growing GST films, where the stoichiometric GST films on the TiN and TiO_2 substrates crystallized well due to the coincidence of crystallization and growth temperature. Meanwhile, the nonstoichiometric GST films on SiO_2, Si_3N_4, and ZrO_2 substrate showed a delayed crystallization behavior. The nucleation density was increased because of the formation of a GeO_2 phase and the charge exchange effect of the partially reduced Ti-oxide on the TiO_2 substrate. On the other hand, the severe incorporation of oxide materials into the growing film could suppress the crystallization of GST nuclei on the SiO_2 surface. The temperature dependence of the saturated growth rate of the GST film suggests that the surface reaction was enhanced by the plasma power, irrespective of the type of substrate. However, the pre-exponential factor was largely dependent on the crystallization of the growing film surface. It is believed that the crystallized GST surface decreased the activation energy for the chemisorption of the precursors and provided the growing film with the necessary charge exchange, which enhanced the saturated growth rate. Although the substrate dependent nucleation and growth behavior has been investigated extensively in many metal CVD processes, the dependence of the saturated growth rate on the crystallinity of the growing film has not been reported. These experimental results are a very unique case of multicomponent film growth where the coincidence of the crystallization and growth temperatures has a key influence on the crystalline quality and accompanying electrical conductivity on the growth rate itself. This appears to be one of the most unique aspects of the CVD/ALD processes of phase changing chalcogenide compounds.

Acknowledgment. The authors acknowledge the support of the National Research Program for the Nano Semiconductor Apparatus Development sponsored by the Korea Ministry of Knowledge and Economy, and World Class University program through the Korea Science and Engineering Foundation funded by the Ministry of Education, Science and Technology (R31-2008-000-10075-0).

CM803369B